Robotica (2014) volume 32, pp. 551–570. © Cambridge University Press 2013
doi:10.1017/S0263574713000866

Stable walking control of a 3D biped robot with foot rotation

Ting Wang, Christine Chevallereau* and David Tlalolini

IRCCyN, CNRS, Ecole centrale de Nantes, 1 rue de la Noë, 44321 Nantes Cedex 03, France

(Accepted August 2, 2013. First published online: September 4, 2013)

SUMMARY

In order to obtain a more human-like walking and less energy consumption, a *foot rotation phase* is considered in the single support phase of a 3D biped robot, in which the stance heel lifts from the ground and the stance foot rotates about the toe. Since there is no actuation at the toe, a walking phase of the robot is composed of a fully actuated phase and an under-actuated phase. The objective of this paper is to present an asymptotically stable walking controller that integrates these two phases. To get around the under-actuation issue, a strict monotonic parameter of the robot is used to describe the reference trajectory instead of using the time parameter. The overall control law consists of a zero moment point (ZMP) controller, a swing ankle rotation controller and a partial joint angles controller. The ZMP controller guarantees that the ZMP follows the desired ZMP. The swing ankle rotation controller assures a flat-foot impact at the end of the swinging phase. Each of these controllers creates two constraints on joint accelerations. In order to determine all the desired joint accelerations from the control law, a partial joint angles controller is implemented. A word "partial" emphasizes the fact that not all the joint angles can be controlled. The outputs controlled by a partial joint angles controller are defined as a linear combination of all the joint angles. The most important question addressed in this paper is how this linear combination can be defined in order to ensure walking stability. The stability of the walking gait under closed-loop control is evaluated with the linearization of the restricted Poincaré map of the hybrid zero dynamics. Finally, simulation results validate the effectiveness of the control law even in presence of initial errors and modelling errors.

KEYWORDS: Bipeds; Control of robotic systems; Humanoid robots; Robot dynamics; Legged robots.

1. Introduction

Compared to human walking, the walking of most existed biped robots looks awkward and has less energetic efficiency. The *foot rotation phase*, where the stance heel lifts from the ground and the stance foot rotates about the toe, allows robot to reduce significantly the cost criterion for fast motions.[12,32] Work in ref. [21] shows that plantarflexion of the ankle, which initiates heel rise and toe roll, is the most efficient method to reduce energy loss at the subsequent impact of the swing leg. This motion is also necessary for the aesthetics of mechanical walking. Thus, it is extremely important and interesting to study the walking control of a humanoid robot with rotation of the feet.

For walking gaits that include foot rotation, various *ad hoc* control solutions have been proposed in the previous literatures. For example, in ref. [29] the robot is controlled to track desired trajectories during foot rotation phase. The toe is modelled as a free joint because the input torque cannot be applied to the toe. This kind of model becomes a non-holonomic constraint system, of which the degree of freedom degenerates. Yi[40] proposed a walking control law for a biped robot with a compliant ankle mechanism. A pseudo-static walking gait with dynamic gait modification method is presented by adjusting the position of a hip joint. The controller has two feedbacks, inner feedback for motor

* Corresponding author. E-mail: Christine.Chevallereau@irccyn.ec-nantes.fr

https://doi.org/10.1017/S0263574713000866 Published online by Cambridge University Press

control and outer feedback for reference trajectory control. Besides, many related works considered the foot rotation phase in the jumping control[8,13] or the running control of the robots.[16] However, none of them can guarantee stability in the presence of the under-actuation that occurs during heel roll or toe roll. Therefore, the aim of our control law is to solve the problem of under-actuation and obtain the stable walking.

To get around the under-actuation issue, the virtual constraints method was proposed. It uses a strict monotonic parameter of the robot to describe the reference trajectory instead of using the time parameter. In the previous work about the control of under-actuated biped robots with point feet,[3,5,9,26] this method was used successfully to solve the under-actuation problem. Next in ref. [4], it is applied for a 2D biped robot with foot rotation at the first time. It is shown that it is also effective for the under-actuation problem during the foot rotation phase. As a following work, in this paper the virtual constraints method is extended to a 3D biped robot with arms and foot rotation. Compared with our previous work,[4] the control law presented in this paper has been modified to avoid a landing of the swing foot with an incorrect orientation with respect to the ground, and to take into account the evolution of the robot in the frontal plane and the coupling between frontal and sagittal plane.

The walking of biped robot is composed of different phases such as single support (SS) with flat-foot, SS with foot rotation around the metatarsal axis and double support (DS)... During every walking phase there is a corresponding dynamic model and contact with the ground. Thus, an appropriate control law has to be implemented for each phase. Generally, the sequence of type of contact with the ground is imposed but it is obtained only if the conditions of ground reaction force, friction cone and zero moment point (ZMP) are satisfied. Most of the recent researches of walking control strategies use ZMP and they are divided into two approaches generally. One method is the periodical replaying of trajectories for the joint motions recorded in advance,[34] which are then applied to the real robot with a little on-line modification.[10,11,20] This strategy explicitly divides the problem into subproblems of planning and control. Another method generates a joint-motion in real time, feeding back the present state of the system to be in accordance with the pre-provided goal of the motion, where planning and control are managed in a unified way.[6,7,17,23,28,30] Two of the more famous users of these methods are Honda Robot Asimo[10] and Kawada's humanoid HRP-2.[15,18]

Almost all the on-line walking controllers are applied to compensate for the ZMP error. However, the general weakness of the previous methods is that they require considerable experimental hand tuning and the proposed methods are poorly documented. The control law proposed in this paper belongs to the first family of methods. The reference trajectory of the joint angles and ZMP have been off-line computed in ref. [33]. Our objective is to propose a new control law to satisfy the constraint of contact and to study the stability of walking, that is, the convergence of periodical walking.

The proposed control law consists of a ZMP controller, a swing ankle rotation controller and a partial joint angles controller. In the ZMP controller, two positions of ZMP in the horizontal plane are regulated to the desired ZMP. This controller produces two dynamic constraints about the joint angle, its velocity and acceleration. Walking on flat ground is considered and the reference trajectory was planned to satisfy the condition of that the robot touches the ground with flat-foot, the swing ankle rotation controller is used to guarantee that the swing foot will touch the ground with flat-foot. It regulates the pitch and roll angle of the swing foot to be their desired values. This controller also produces two dynamic constraints. Consequently, for a 3D robot with n actuated joints, since two positions of ZMP and two rotation angles of the swing ankle are controlled, only other $n-4$ controlled outputs can be chosen. For simplicity, the $n-4$ controlled outputs, which is written as u, are defined as a linear combination of the n actuated joints. The partial joint angles controller is applied to make u track its desired value u^d. As a result, the three controllers produce n dynamic equations to determine the acceleration of n actuated joints, then the input torque can be obtained by the inverse dynamics. The choice of controlled outputs u involved in the partial joint angles controller affects the stability of the walking gait under closed-loop control. Thus, the controlled outputs u are chosen in order to have stable walking. The stability is evaluated with the linearization of the restricted Poincaré map of the hybrid zero dynamics[39] like in our previous studies,[5,36] involving planar biped robot with under-actuated ankle joints.

In short, the ZMP controller and swing ankle controller are used to ensure the stable ground contact of stance foot and correct landing of the swing foot, respectively. The partial joint angles controller is used to track the reference trajectory and satisfy the stability condition of the overall control law

https://doi.org/10.1017/S0263574713000866 Published online by Cambridge University Press

in the sense of the convergence towards a cyclic motion. The three controllers have been validated in the control of a 3D biped robot without arms and foot rotation.[37] Here it is extended to a more complicated robot model and the foot rotation phase, which is under-actuated, is considered. By regarding the foot rotation angle as an actuated joint angle and considering all of its effects on the dynamic models of robot, a control law is proposed for both fully actuated phase and the foot rotation phase. Compared to the general control law in the recent studies, our control law has some advantages as follows. The proposed method can be viewed as an on-line modification of the reference trajectory in order to ensure the satisfaction of the constraint of contact. The main point is that the effect of this on-line modification on the stability of walking is studied based on rigorous stability analysis, not by testing on the robot which requires considerable experimental hand tuning. More importantly, the stability during the foot rotation phase can also be taken into account, that is exactly what is missing in previous studies for walking gaits with foot rotation.

This paper is organized as follows. Section 2 is a description of the biped robot and its dynamic models during different walking phases. Since the parameterized reference trajectory will be used to solve the under-actuation problem during the foot rotation phase, the parameterization of the reference trajectory of the joint angles and ZMP is introduced in Section 3. Section 4 introduces the principle of control law including ZMP controller, swing ankle rotation controller and partial joints controller, and it also introduces the modification of the reference motion after the impact phase to create a continuous and cyclic desired trajectory. In Section 5, the hybrid zero dynamic is detailed and stability analysis based on the Poincaré method is proposed. In order to show its validity, the simulation results of the control law considering initial errors and modelling errors are given in Section 6. Concluding remarks are made in Section 7.

2. Model

2.1. Biped model

The study of this robot is supported by R2A2 project of ANR. The robot's model is shown in Fig. 1.[2] The 3D robot is comprised of a torso, two identical arms and legs with feet. All links are assumed to be massive and rigid. The inertia of each link is also taken into account. All the parameters of the robot in detail are shown in ref. [35].

The studied robot has 28 degrees-of-freedom: three at pelvis and each ankle, hip and shoulder, one at torso and each knee, elbow and toe of each foot. In fact, for the swing foot, the rotation of the toe is not needed in the walking control so it is not considered here. As a result, the joints' configurations used in the dynamic model are written as

$$q = [q_1, \ldots, q_{27}]^T_{27\times 1} \tag{1}$$

and they are defined as shown in Fig. 1, where the coordinate system x_s, y_s, z_s is fixed on the ground and is referred as the absolute coordinate system.

Note that q_1 describes the rotation angle of the stance toe in the sagittal plane and we suppose that it can be measured or estimated for the real robot. Since there is no actuation at the toe, only the last 26 joints' configurations in q are actuated and the vector of actuated variables is written as

$$q_a = [q_2, \ldots, q_{27}]^T_{26\times 1}. \tag{2}$$

Similarly, the torque vector considered has 26 components corresponding to q_a:

$$\Gamma = [\Gamma_2, \ldots, \Gamma_{27}]^T_{26\times 1}. \tag{3}$$

When the stance foot contacts the ground completely and is stationary $q_1 = 0, \dot{q}_1 = 0, \ddot{q}_1 = 0$, the centre of pressure (CoP) of the forces on the foot remains strictly within the interior of the footprint. The system is fully actuated. In the foot rotation phase, the CoP moves to the toe, that allows the foot to rotate, $q_1 \neq 0, \dot{q}_1 \neq 0, \ddot{q}_1 \neq 0$, thus the system is now under-actuated.

https://doi.org/10.1017/S0263574713000866 Published online by Cambridge University Press

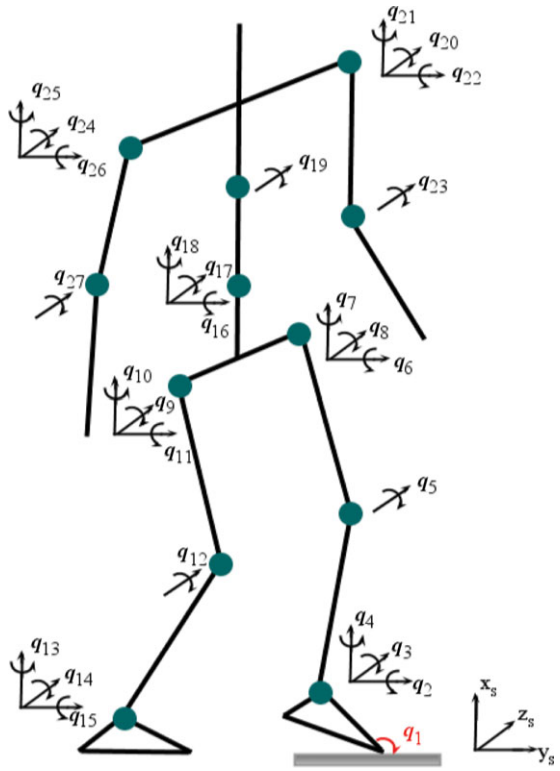


Fig. 1. (Colour online) Biped model.

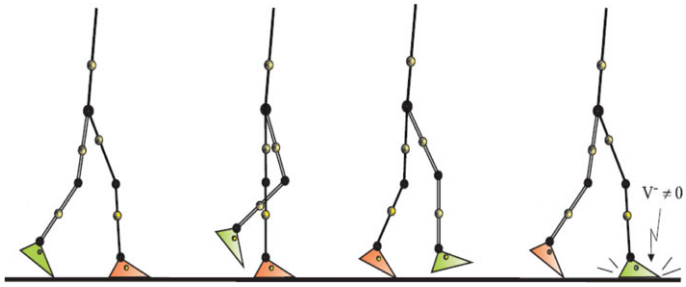


Fig. 2. (Colour online) Walking gait of the studied robot with the foot rotation phase. Adapted from ref. [33].

2.2. Dynamic model

A whole walking phase of the studied robot is shown in Fig. 2. The walking begins from an instantaneous double support phase, during which one foot touches the ground completely and the other one is preparing to lift and only its toe touches the ground. The following single support phase is divided into the fully support phase and the foot rotation phase. At the end of the foot rotation phase, the swing foot parallels to the ground and then the impact occurs.

The dynamic models for every walking phase are derived here by assuming support on left leg. They are described as follows and the models for support on right leg can be written in a similar way. It is worth mentioning that the models to be proposed are suitable for both of the fully support phase and the foot rotation phase.

2.2.1. Dynamic model of single support phase. The Newton Euler algorithm is used to calculate the dynamic model of a 3D biped robot during the single support phase.[31,33] The actuator torques and the ground reaction (forces and moments) to the stance foot can be computed as soon as the joint position, velocity and acceleration q, $\dot{q}$, $\ddot{q}$ are known, and they are linear functions of the acceleration

https://doi.org/10.1017/S0263574713000866 Published online by Cambridge University Press

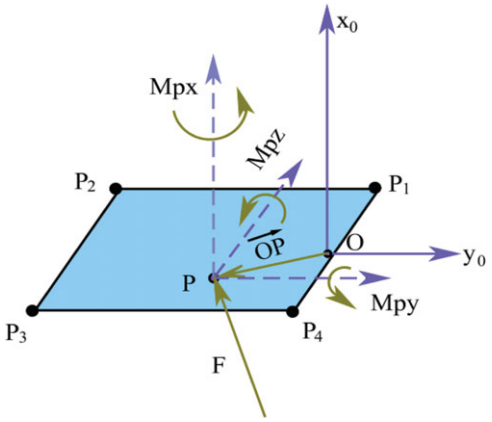


Fig. 3. (Colour online) The support foot.

$\ddot{q}$. Consequently, the dynamic model is represented as

$$\begin{bmatrix} F \\ M \\ \Gamma \end{bmatrix} = NE(q, \dot{q}, \ddot{q}) = NE_1(q)\ddot{q} + NE_2(q, \dot{q}), \tag{4}$$

where $NE_1(q)$ denotes all the coefficient terms of $\ddot{q}$ and $NE_2(q, \dot{q})$ denotes all the terms without $\ddot{q}$ and it includes Coriolis, centrifugal and gravitational terms. F and M compose the wrench vector exerted by the ground on the stance foot and they will be used to calculate the position of ZMP. They are expressed in the set of coordinate x_0, y_0, z_0 that is fixed at the left leg. The calculation of the torque vector Γ will be used in the control law.

Not any desired acceleration will produce admissible reaction force i.e. reaction force satisfying the hypothesis of contact and especially the hypothesis about the position of the ZMP. This constraint is particularly severe during the foot rotation phase, where ZMP_x must be 0.

2.2.2. ZMP dynamics. When the leg-1 is on the ground, a ground reaction force and moment can be expressed about any point in the support plane. If a point P is in the plane of the foot-1 (see Fig. 3), the ground reaction moment M_p of P can be calculated by

$$M_p = M - \vec{OP} \times F, \tag{5}$$

where $\vec{OP}$ is the distance vector of the point P in the reference frame x_0, y_0, z_0. Considering F, M are functions of $q, \dot{q}, \ddot{q}$ and linear functions of the acceleration $\ddot{q}$ (see Eq. (4)), the components of M_p along the axes y_0 and z_0 can be written as

$$\begin{bmatrix} M_{py} \\ M_{pz} \end{bmatrix} = f(q, \dot{q}, \ddot{q}, \vec{OP}) = W\ddot{q} + H, \tag{6}$$

where the function $f(\cdot)$ in Eq. (6) depends on Eqs. (4) and (5), and W, H can be obtained by:

$$H = f(q, \dot{q}, \ddot{q} = \mathbf{0}_{27\times1}, \vec{OP}), \tag{7}$$

and

$$\begin{cases} W(:, i) = f(q, \dot{q}, \ddot{q} = \mathbf{e}_{27\times1}, \vec{OP}) - H \\ \mathbf{e}(i) = 1, \quad i \in \{1, 2, \ldots, 27\} \\ \mathbf{e}(j) = 0, \quad j \in \{1, 2, \ldots, 27\} \quad \textit{and} \quad j \neq i \end{cases}. \tag{8}$$

https://doi.org/10.1017/S0263574713000866 Published online by Cambridge University Press

According to the definition of ZMP, if P is ZMP, the horizontal ground reaction moment of the ground reaction force about this point equals to zero. Thus, Eq. (6) can be used to constrain the ZMP which is such that:

$$M_{py} = M_{pz} = 0 \tag{9}$$

to be a desired point P.

Remark: When the foot is flat on the ground, frame x_0, y_0, z_0 attached to the ground and frame x_1, y_1, z_1 attached to the sole of the foot coincide. When the foot rotates, only position of the ZMP such that $\vec{OP}$ is aligned with $z_0 = z_1$ will be considered, since the ZMP belongs to the contact area between the ground and the sole of the stance foot.

2.2.3. Dynamic model of impact phase. During the impact, the biped's configuration variables do not change, but the generalized velocities undergo a jump. As shown in ref. [39], this jump is linear with respect to the joint velocity before the impact. The index $-$ and $+$ are used to distinguish the values just before and after impact, respectively. Since the stance foot touches the ground completely after impact, $q_1^+ = 0$ and $\dot{q}_1^+ = 0$, thus only the states of actuated joints $q_a, \dot{q}_a$ need to be calculated in the impact model and they are given by

$$\begin{cases} {q_a}^+ = E{q_a}^- \\ {\dot{q}_a}^+ = EI(q^-)\dot{q}^- \end{cases}, \tag{10}$$

where $E_{26\times 26}$ is a permutation matrix describing exchanges of legs and arms. The function $I_{26\times 27}$ represents the linear jump of the joint velocity.

3. Parameterization of the reference trajectory

A reference trajectory of joint angles and ZMP described as function of time $q^d(t)$, $ZMP^d(t)$ have been calculated off-line through the minimization of the energy consumption.[33] During the foot rotation phase, if the tracking requirements of the control law were posed in the time domain, the walking system would be under-actuated in the sense that the number of inputs would be less than the number of independent degrees-of-freedom. In order to solve this problem, q^d could be parameterized by a quantity depending on the state of the robot that is strictly monotonic like time t during the walking phase. This method has been used successfully for the walking of bipeds with point feet[3,5,26,38] and the walking of planar biped with foot rotation.[4] Therefore, it is still used here and the parameterized reference trajectory is given as follows.

In a forward walking motion, if a virtual stance leg is defined by the line that connects the stance foot to the stance hip, the angle of this leg in the sagittal plane denoted by θ is monotonic and it can replace the time t to parameterize q^d and ZMP^d.

As shown in Fig. 4, this angle is considered as referenced to the initial frame, and hence is an absolute angle. Because the shin and the thigh have the same length, it can be calculated as

$$\theta = 0.5q_3 + 0.5q_5 - q_1. \tag{11}$$

For flat-foot phase and the foot rotation phase, we choose θ to parameterize the reference trajectory, it is not only strictly monotonic during the walking phase, but it is also a linear function of the vector of joint angle q, thus it can be easily used in the control law.

Next a reference path $h^d(\theta)$ is designed in order to be compatible with a periodic solution of the biped model. It must satisfy

$$\begin{cases} q^d(t) = h^d(\theta) \\ \dot{q}^d(t) = \frac{\partial h^d(\theta)}{\partial \theta}\dot{\theta} \\ \ddot{q}^d(t) = \frac{\partial^2 h^d(\theta)}{\partial \theta^2}\dot{\theta}^2 + \frac{\partial h^d(\theta)}{\partial \theta}\ddot{\theta} \end{cases}. \tag{12}$$

According to a known reference trajectory $q^d(t)$, $\dot{q}^d(t)$, $\ddot{q}^d(t)$, using Eqs. (12) and (11), $h^d(\theta)$, $\frac{\partial h^d(\theta)}{\partial \theta}$ and $\frac{\partial^2 h^d(\theta)}{\partial \theta^2}$ can be deduced and they are assumed to be known in the following contents. Similarly, the

https://doi.org/10.1017/S0263574713000866 Published online by Cambridge University Press

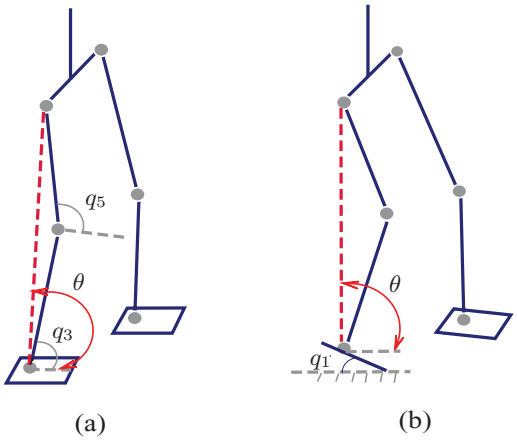


Fig. 4. (Colour online) The definition of θ during the fully support phase (a) and the foot rotation phase (b). θ defines the orientation of the dotted line (in red) connecting the stance ankle and stance hip in the sagittal plane.

known reference trajectory $ZMP^d(t)$ is written as $ZMP^d(\theta)$. Here and in the following subsections, the superscript d denotes the desired value.

4. A control law considering ground contact and stability

The proposed control consists of a ZMP controller, a swing ankle rotation controller and a partial joint angles controller. The former two controllers are used to achieve $ZMP = ZMP^d(\theta)$ and make the swing foot keep flat at impacts respectively, which are helpful to ensure the stable contact. The third controller implements the joint path control and it is partial since the torques are already partially defined by the former two controllers. In addition, in order to create a continuous and cyclic desired trajectory, the reference motion is modified after the impact phase. In this paper, since the rotation angle of the stance foot in the sagittal plane, i.e., q_1, has been considered in the joints' configurations vector q, it must be included in the partial joint angles controller although it is not actuated. The non-actuation of this joint is treated in the control of the ZMP position.

4.1. ZMP controller

The objective of this controller is to have

$$ZMP = ZMP^d(\theta). \tag{13}$$

According to the definition of ZMP, Eq. (6) can be rewritten as

$$W(q, \dot{q})\ddot{q} + H(q, \dot{q}) = \mathbf{0}_{2\times 1}, \tag{14}$$

where W and H are recalculated by Eqs. (7) and (8) with $\vec{OP} = ZMP^d(\theta)$.

4.2. Swing ankle rotation controller

We assume that the reference trajectory q^d, $\dot{q}^d$, $\ddot{q}^d$ has been defined such that the sole of the transferred foot is parallel to the ground at each impact phase. Since not all the joint angles q are controlled directly in our control law, the swing ankle rotation is developed to force the pitch and roll angle of the swing foot to be their desired values, and in particular to be zero at impact. As a result, the robot will touch the ground with flat- foot and the next impact will occur in a good way.

In Fig. 1, the angles q_{13}, q_{14} and q_{15} are used to describe the relative orientation of the swing ankle. They reflect respectively the yaw, pitch and roll movement of the swing foot. Therefore, in order to control the pitch and roll movement of the swing foot to force it keep flat just before impact, the previous 15 joints should be constrained. Let ${}^sR_{15}$ be a 3×3 orientation matrix from the absolute

https://doi.org/10.1017/S0263574713000866 Published online by Cambridge University Press

coordinate system x_s, y_s, z_s to the coordinate system of the 15th joint x_{15}, y_{15}, z_{15}:

$$^{s}R_{15} = [s, n, a]_{3\times 3}, \tag{15}$$

where $s_{3\times 1}$, $n_{3\times 1}$ and $a_{3\times 1}$ are unitary vectors defining x_{15}, y_{15}, z_{15} in frame R_s, respectively.

Next $^{s}R_{15}^{d} = [s^d, n^d, a^d]$ is used to denote the desired orientation of transformation matrix $^{s}R_{15}$ with the reference trajectory q^d. If there exists a tracking error between q and q^d, there will be a small error in the orientation of the swing ankle which can be defined as ξ[22]

$$\xi = \frac{1}{2}(s \times s^d + n \times n^d + a \times a^d). \tag{16}$$

The derivatives of the orientation error are

$$\begin{cases} \dot{\xi} = {}^{s}\omega_{15}{}^{d} - {}^{s}\omega_{15} \\ \ddot{\xi} = {}^{s}\dot{\omega}_{15}{}^{d} - {}^{s}\dot{\omega}_{15} \end{cases}, \tag{17}$$

where $^{s}\omega_{15}$ and $^{s}\dot{\omega}_{15}$ are the angular velocity and acceleration of the joint 15 in the absolute coordinate system $x_s y_s z_s$. They can be efficiently computed by the forward recursive equations of the general serial robot with $q_1, \ldots, q_{15}$, their velocity and acceleration.[19]

Because only the pitch and roll angle of swing foot need to be regulated, that means the orientation of swing ankle around the x_s direction is not necessary, thus the objective of this control law is

$$\xi_{yz} = \mathbf{0}_{2\times 1.} \tag{18}$$

Here and in the following subsections, the subscript yz denotes the last two lines of the vector, which correspond to the rotation around the y_s direction and the z_s direction, respectively. Equation (18) can be achieved by a PD correction:

$$\ddot{\xi}_{yz} + \frac{K_1}{\varepsilon}\dot{\xi}_{yz} + \frac{K_2}{\varepsilon^2}\xi_{yz} = \mathbf{0}_{2\times 1}, \tag{19}$$

with $K_1 > 0$, $K_2 > 0$, and $\varepsilon > 0$. Equation (19) offers two restriction equations about $q, \dot{q}, \ddot{q}$ and they can be rewritten as Eq. (14):

$$W_s(q, \dot{q})\ddot{q} + H_s(q, \dot{q}) = \mathbf{0}_{2\times 1}, \tag{20}$$

where $W_s(q, \dot{q})$ denotes all the coefficient terms of $\ddot{q}$ and $H_s(q, \dot{q})$ denotes all the terms without $\ddot{q}$ in Eq. (19).

4.3. Partial joint angles controller

The proposed control law is a computed torque control, thus 27 equations about the states of robot have to be obtained to determine the desired acceleration $\ddot{q}_{27\times 1}$ used in the calculation of torques Γ. Since Eqs. (13) and (18) have offered four restrictions about the states of robot $q, \dot{q}, \ddot{q}$, other 23 controlled outputs can be chosen. Thus, how to choose these 23 controlled outputs from the 27 joints is presented at first.

Because the pitch and roll movement of the swing foot are actuated by the 14th and 15th joint (see Fig. 1), so we can suppose that q_{14} and q_{15} have been constrained by the swing ankle rotation controller using $q_1, q_2, \ldots, q_{13}$. Thus, there is no need to consider them again in the partial joint angles controller. In addition, because all the reference trajectories are parameterized by θ and $\theta = 0.5q_3 + 0.5q_5 - q_1$, q_3, q_5 and q_1 are not independent of each other so q_3 is excluded here. Therefore, the joint angles that are not directly controlled via the parameterization of the reference trajectory and the swing ankle controller are

$$Q_r = [q_1, q_2, q_4, q_5, \ldots, q_{13}, q_{16}, \ldots, q_{27}]^{T}_{24\times 1,} \tag{21}$$

https://doi.org/10.1017/S0263574713000866 Published online by Cambridge University Press

where Q_r has 24 elements but only 23 controlled outputs can be defined. Since the second joint influences the lateral position of ZMP directly, in order to distinguish q_2 from other joints in Q_r and avoid singularity in the control law, the controlled joint angles are chosen as

$$u = Q + M_1 q_2 \tag{22}$$

with

$$Q = [q_1, q_4, q_5, \ldots, q_{13}, q_{16}, \ldots, q_{27}]^T_{23\times 1.} \tag{23}$$

The previous studies[5,36] have shown that the choice of controlled joints affects the stability of the walking, thus the stability condition will be a criteria to select M_1. Therefore, here M_1 is a 23×1 constant matrix to be determined by the stability analysis. The objective of the partial joint angles controller is to regulate u to track its desired value $u^d(\theta)$. It is achieved by a PD correction such as (19):

$$\ddot{u} - \ddot{u}^d + \frac{K_d}{\varepsilon}(\dot{u} - \dot{u}^d) + \frac{K_p}{\varepsilon^2}(u - u^d) = \mathbf{0}_{23\times 1}, \tag{24}$$

where u^d, $\dot{u}^d$, $\ddot{u}^d$ can be calculated using the definition of u in Eq. (22) and the referenced trajectory q^d, $\dot{q}^d$, $\ddot{q}^d$ in Eq. (12). Because u is a linear function of the joint angles q (see Eq. (22)), obviously, $\ddot{u}$ in Eq. (24) is a linear function of $\ddot{q}$, so Eq. (24) can be written in the same format as Eqs. (14) and (20):

$$W_j(q, \dot{q})_{23\times 27}\ddot{q} + H_j(q, \dot{q})_{23\times 1} = \mathbf{0}_{23\times 1}, \tag{25}$$

where $W_j(q, \dot{q})$ denotes all the coefficient terms of $\ddot{q}$ and $H_j(q, \dot{q})$ denotes all the terms without $\ddot{q}$ in (24).

4.4. Modification of the tracked errors caused by impact

Based on the proposed three controllers, the desired properties respectively are

$$\begin{cases} y_1 = ZMP - ZMP^d(\theta) = \mathbf{0}_{2\times 1} \\ y_2 = \xi_{yz} = \mathbf{0}_{2\times 1} \\ y_3 = u - u^d(\theta) = \mathbf{0}_{23\times 1} \end{cases}. \tag{26}$$

These controllers act for each single support phase only and the impact is passive. The original reference trajectory is defined by taking into account the impact phase. If the desired states of robot can be achieved before the impact, they will be achieved after the impact. The impact condition is a geometric condition. Thus, it can occur with some errors, especially with some errors on θ and q_2 because they are not controlled directly as other states in u. As a result, large errors on the joint position and velocity will be created after impact, that means discontinuity of errors will exist.

In order to avoid the discontinuity, and large torque that can perturb the contact with the ground, the reference trajectory in Eq. (26) is modified stride to stride so that they are compatible with the initial state of the robot at the beginning of each step.[5] It is not necessary to modify $ZMP^d(\theta)$ because the position of ZMP acts directly at the acceleration level where the discontinuities are acceptable. The new output for the feedback control design is

$$\begin{cases} y_1 = ZMP - ZMP^d(\theta) = \mathbf{0}_{2\times 1} \\ y_{2c} = \xi_{yz} - \xi_{yzc} = \mathbf{0}_{2\times 1} \\ y_{3c} = u - u^d(\theta) - u_c = \mathbf{0}_{23\times 1} \end{cases}. \tag{27}$$

Here, ξ_{yzc} and u_c are modification terms of the original reference motions. Their calculation is presented as follows.

The function u_c is taken to be a fourth-order continuously differentiable function of θ:

$$u_c = a_0 + a_1\theta + a_2\theta^2 + a_3\theta^3 + a_4\theta^4, \tag{28}$$

https://doi.org/10.1017/S0263574713000866 Published online by Cambridge University Press

where the coefficients $a_0, \ldots, a_4$ are defined such that[1]

$$\begin{cases} u_c(\theta_i) &= y_{3i} \\ \frac{\partial u_c}{\partial \theta}(\theta_i) &= \frac{\dot{y}_{3i}}{\dot{\theta}_i} \\ u_c(\theta) &\equiv 0, \quad \theta \geq \frac{\theta_i+\theta_f}{2}, \end{cases} \tag{29}$$

where y_{3i} and $\dot{y}_{3i}$ denote the initial values of y_3 and $\dot{y}_3$, and they are updated at the beginning of the step and held constant throughout the step. Specifically, $y_{3i} = u_i - u^d(\theta_i)$ and $\dot{y}_{3i} = \dot{u}_i - \dot{u}^d(\theta_i)$. Here, θ_i and θ_f are the initial and final value of θ respectively, and they can be calculated by Eq. (11) using q_i to q_f. By using u_c defined in this way, the new reference trajectory starting from the current state just after the impact is smoothly joined to the original reference trajectory at the middle of the step. In particular, for any initial error, the initial reference trajectory u^d is not modified in the second part of the step : $\theta \geq \frac{\theta_i+\theta_f}{2}$.

Similarly, the function of ξ_{yzc} in Eq. (27) is defined in the same format as Eq. (28) and all the coefficients are determined using the value of y_2 in Eq. (26) and its derivative at the beginning of each step. As a result, these modification terms are supplemented in the PD correction expressions (19) and (24):

$$\ddot{\xi}_{yz} - \ddot{\xi}_{yzc} + \frac{K_1}{\varepsilon}(\dot{\xi}_{yz} - \dot{\xi}_{yzc}) + \frac{K_2}{\varepsilon^2}(\xi_{yz} - \xi_{yzc}) = \mathbf{0}_{2\times 1}, \tag{30}$$

$$\ddot{u} - \ddot{u}^d - \ddot{u}_c + \frac{K_d}{\varepsilon}(\dot{u} - \dot{u}^d - \dot{u}_c) + \frac{K_p}{\varepsilon^2}(u - u^d - u_c) = \mathbf{0}_{23\times 1}. \tag{31}$$

4.5. Torque calculation

With the proposed three controllers, 27 equations about $q, \dot{q}, \ddot{q}$ are obtained by Eqs. (14), (20) and (25), and they are linear functions of $\ddot{q}$. Considering the impact modifications, the latter two controllers (20) and (25) are recreated using Eqs. (30) and (31) to satisfy Eq. (27), and they are also linear functions of $\ddot{q}$. Thus, 27 new equations about $q, \dot{q}, \ddot{q}$ can be combined as

$$A(q, \dot{q})\ddot{q} + B(q, \dot{q}) = \mathbf{0}_{27\times 1}. \tag{32}$$

Next, the $\ddot{q}$ is resolved directly:

$$\ddot{q} = -A^{-1}B. \tag{33}$$

For the proposed choice of u defined by (22), no singularity appears in simulation for the inversion of matrix A. Then, the desired torques Γ can be calculated with $\ddot{q}$, $\dot{q}$ and q by the inverse dynamics via the Newton Euler algorithm (4). It can be noticed that the acceleration defined by Eq. (33) is compatible with the contact hypothesis since condition on ZMP is satisfied; thus, the torque around q_1 in the foot rotation phase is naturally zero.

5. Stability analysis

The stability of the control law is defined in the sense of the convergence towards a periodic motion. Refs. [3, 5, 26, 38] and [39, Chap. 4] have proposed that the stability of the closed-loop system can be studied in a reduced-dimensional state space based on hybrid zero dynamics (HZD). For a system modelled by ordinary differential equations (in particular, without impact dynamics), the maximal internal dynamics of the system that is compatible with the output being identically zero is called the zero dynamics.[14,25] HZD is a zero dynamics of the full hybrid model, i.e., the dynamics at impact is included.

[1] The four-order polynomial is used for $\theta_i \leq \theta \leq \frac{\theta_i+\theta_f}{2}$; Continuity of position, velocity and acceleration are ensured at $\theta = \frac{\theta_i+\theta_f}{2}$.

https://doi.org/10.1017/S0263574713000866 Published online by Cambridge University Press

5.1. Reduction of the states dimension using HZD

A restricted Poincaré map is defined from $S_\theta \cap Z$ to $S_\theta \cap Z$, where $Z = \{(\theta, q, \dot{q}) | y_1 = 0, y_{2c} = 0, \dot{y}_{2c} = 0, y_{3c} = 0, \dot{y}_{3c} = 0\}$ describes the zero dynamics manifold (see Eq. (27)) and $S_\theta = \{(\theta, q, \dot{q}) | \theta = 0.4\theta_i + 0.6\theta_f\}$ is chosen as the Poincaré section because at this instant the swing foot does not touch the ground, and since $\theta \geq \frac{\theta_i^d + \theta_f^d}{2}$, the controlled variables are not affected by u_c and ξ_{yzc} in Eq. (27). Now, we will present how to reduce the states dimension of this system in $S_\theta \cap Z$.

According to the definition of HZD, the Eq. (27) is supposed to be realized by the proposed control law. Therefore, based on the swing ankle rotation controller and partial joint angles controller which are described as the last two sub-equations in Eq. (27), we have

$$\begin{cases} [q_{14}, q_{15}] = f_\xi(q_1, q_2, \ldots, q_{13}) \\ Q = u^d(\theta) - M_1 q_2 \end{cases}, \tag{34}$$

where f_ξ expresses the solution of q_{14}, q_{15} to achieve $\xi_{yzc} = \xi_{yzc}^d = 0$ as function of q_1, q_{13}.

By using Eq. (34) and the definition of u, Q and θ, the state of robot q can be described by θ, q_2, M_1, q^d, where M_1 and q^d are known vectors. Consequently, a simplified expression of $q, \dot{q}$ is defined by a function f_{HZD}:

$$[q, \dot{q}] = f_{HZD}(q_2, \theta, \dot{q}_2, \dot{\theta}, M_1, C_{q^d}), \tag{35}$$

where C_{q^d} denotes all the known terms introduced by the reference trajectory q^d and its derivatives.

The acceleration $\ddot{q}$ can be expressed as a function of $q_2, \theta, \dot{q}_2, \dot{\theta}, \ddot{q}_2, \ddot{\theta}$ and it depends on M_1 and C_{q^d}. Based on that, Eq. (27) corresponds to

$$\begin{cases} W_{HZD}(q, \dot{q}) \begin{bmatrix} \ddot{q}_2 \\ \ddot{\theta} \end{bmatrix} + H_{HZD}(q, \dot{q}) = \mathbf{0}_{2\times 1} \\ [q, \dot{q}] = f_{HZD}(q_2, \theta, \dot{q}_2, \dot{\theta}, M_1, C_{q^d}) \end{cases}, \tag{36}$$

where the first line of Eq. (36) is deduced by the ZMP controller (14). $W_{HZD}(q, \dot{q})$ denotes all the coefficient terms of $\ddot{q}_2$ and $\ddot{\theta}$, and $H_{HZD}(q, \dot{q})$ denotes all the terms without these terms. It clearly shows that the property of the closed-loop system can be analysed using $q_2, \theta, \dot{q}_2, \dot{\theta}$ for the proposed control law for any value of M_1. In fact, in the chosen Poincaré section $\theta = 0.4\theta_i^d + 0.6\theta_f^d$, the Poincaré return map is a function of three independents variables $x = (q_2, \dot{q}_2, \dot{\theta})$ like the 3D biped robot without the foot rotation.[37] Since the periodic reference motion $q^d(t)$ is known, the fixed point of the Poincaré return map is $x^* = ({q_2}^d(\theta^*), \dot{q}_2^d(\theta^*), \dot{\theta}^*(\theta^*))$, and the stability has to be studied around this point x^*.

5.2. Stability analysis

The restricted Poincaré map $P^z : S_\theta \cap Z \to S_\theta \cap Z$ induces a discrete-time system $x_{k+1} = P^z(x_k)$..[24] It states that for ε sufficiently small in Eqs. (30) and (31), *the linearization of P^z about a fixed-point determines exponential stability of the full-order closed-loop robot model*. As soon as a cyclic motion $q^d(\theta)$ is given, a fixed-point x^* is known for the proposed control law for any value of M_1. Define $\delta x_k = x_k - x^*$, the Poincaré map linearized about the fixed-point x^* gives rise to a linearized system,

$$\delta x_{k+1} = A^z \delta x_k, \tag{37}$$

where the (3×3) square matrix A^z is the Jacobian matrix of the Poincaré map, and it can be calculated as shown in ref. [5].

A fixed point of the restricted Poincaré map is locally exponentially stable, if and only if, the eigenvalues of A^z have magnitude strictly less than one (see ref. [39, Chap. 4]).

6. Simulation results

In order to validate the control law proposed above, simulation results are presented in this section.

https://doi.org/10.1017/S0263574713000866 Published online by Cambridge University Press

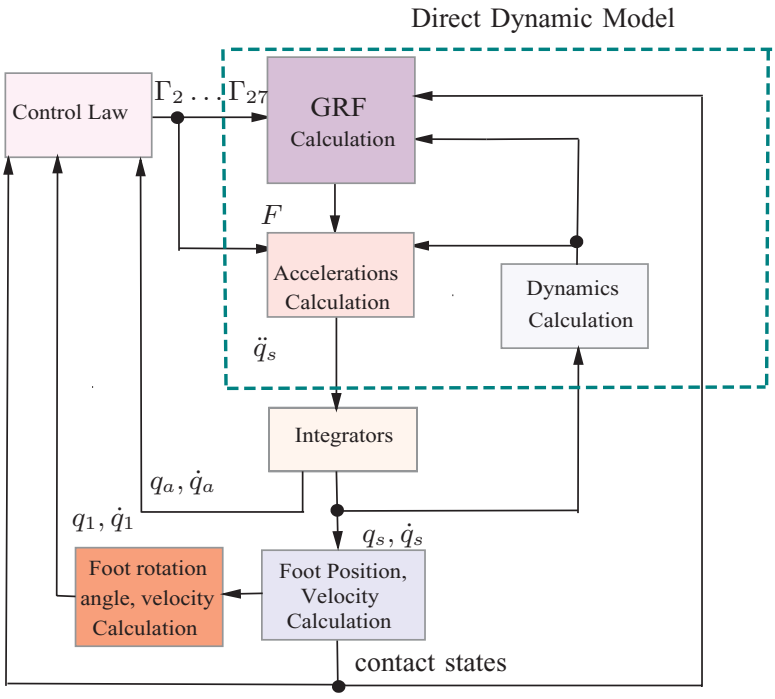


Fig. 5. (Colour online) Block diagram of the simulator for the walking.

6.1. Simulator

The control law is tested on a simulator including a rigid ground model. The simulation is done using the MATLAB–Simulink software and the dynamic model is calculated using the Newton–Euler method and written in C language. The foot is supposed to be rigid and four contact points P_1, P_2, P_3 and P_4 are defined (see Fig. 3) for each foot. If one of these points is in contact with the ground, the corresponding reaction force is computed by solving a linear complementarity problem (LCP).[1] Since the punctual contact at each corner of the foot $P_1, \ldots, P_4$ is considered, the slipping, rolling or take-off of the foot can be modelled. The reduction of the calculation cost of the simulation was not an objective of this study, but the possibility to have a precise modelling of different contact conditions was one of our priority.[27] Since any contact can be considered in the simulator, the configuration of the robot is defined by the actuated joint q_a plus six coordinates that define the position and orientation of the right foot. Thus, the robot is parameterized by a vector $q_s = [X_1, \alpha, q_a]^T$, where X_1 denotes the position of the frame x_1, y_1, z_1 attached to the right foot, and α is the Euler angle that defines the orientation of frame x_1, y_1, z_1 with respect to a fixed frame x_s, y_s, z_s. The foot situation $[X_1, \alpha]$ is not directly used by the control law but it allows to calculate the foot rotation angle q_1 and its velocity $\dot{q}_1$.

The block diagram of the simulator is shown in Fig. 5.

6.2. Reference trajectory

A method to obtain the cyclic optimal walking gait with the foot rotation phase has been proposed in ref. [33]. During the foot rotation phase, the CoP remains strictly on the toe axis of the stance foot to allow the foot to rotate. The synthesis of the reference walking trajectories is stated under the form of a constrained parameter optimization problem. The resolution of this problem is obtained by sequential quadratic programming (SQP) methods. The performance criterion, based on the square of the torques, is optimized in order to increase the autonomy of energy of the biped robot. Furthermore, some constraints, such as actuator performances and limits on the ground reaction force in single support phases and at impacts, are taken into account. The obtained stick diagram for one step of the periodic walking gait is shown in Figs. 6 and 7. From them, we can clearly see that the stance heel lifts from the ground and the stance foot rotates about the toe.

https://doi.org/10.1017/S0263574713000866 Published online by Cambridge University Press

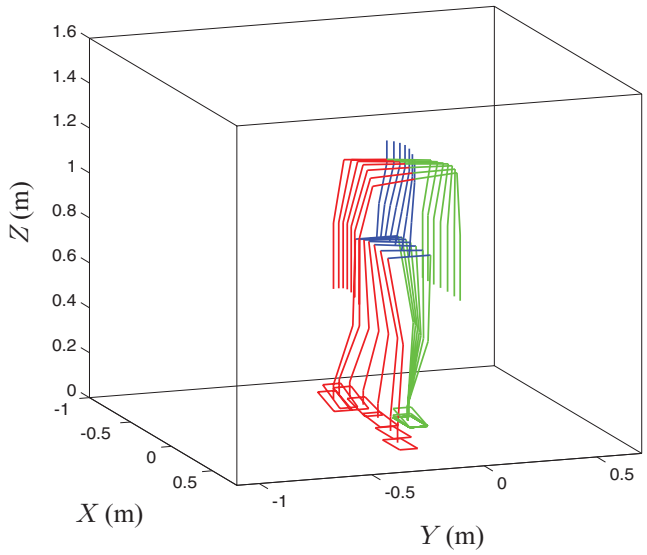


Fig. 6. (Colour online) Stick diagram for one walking step with the foot rotation phase in 3D space.

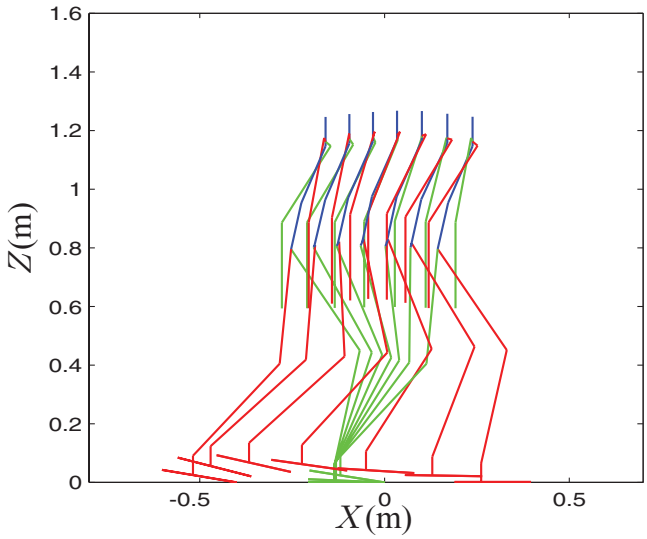


Fig. 7. (Colour online) Stick diagram for one walking step with foot rotation phase in the sagittal plane.

6.3. The effect of different controlled partial joints on the walking stability

In order to ensure the stability of the proposed control, we have many degree-of-freedom in the choice of M_1. The role of this vector is to define the synergy used for the dynamic equilibrium in the frontal plane. The dynamic equilibrium in the sagittal plane is essentially due to θ, meaning thereby a change of the temporal evolution of the desired motion as it has been seen for planar robot.[4] The dynamic equilibrium in the frontal plane allows to define q_2, how the modification of q_2 is reported on the others joints in order to ensure stability must now be defined. In others words, the effect of M_1 on the walking stability should be studied. First of all, we check that for $M_1 = 0_{23\times1}$, the control is not stable, since the maximal norm of the eigenvalue of A^Z is greater than one. Different approaches can be used to define M_1. In ref. [5], an arbitrary synergy based on control of the swing foot is used. The choice of M_1 by optimization to satisfy stability condition is also possible.

In this study, we have chosen to modify only one joint evolution, to reduce the influence of the modification of q_2 on the joint control. An exploration technique is used to illustrate the effect of $M_{1(23\times1)}$, 22 components of M_1 are fixed to zero, then the largest magnitude of the eigenvalues of A^z in Eq. (37) is drawn as functions of the 23th component of M_1. If it is less than 1, the obtained

https://doi.org/10.1017/S0263574713000866 Published online by Cambridge University Press

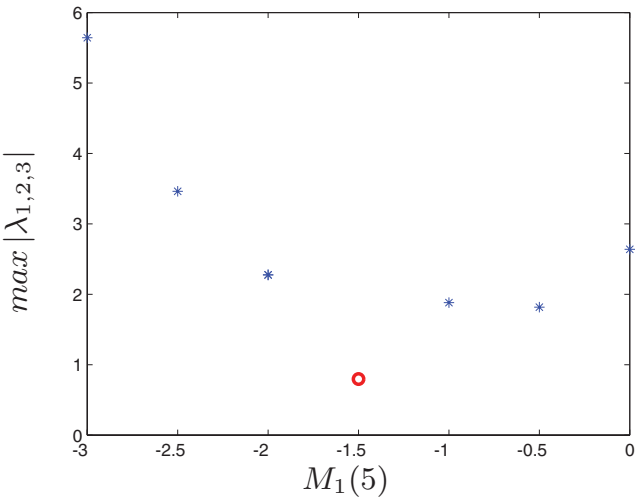


Fig. 8. (Colour online) $max|\lambda_{1,2,3}|$ versus $M_1(5)$, when the other 22 components of M_1 are zero.

walking is stable. Many joints can affect the values of the maximal eigenvalue of A^Z, even the joints of the arms as an effect on the stability. For the case studied, we can classify the joints into three sets. The joints that have a small contribution in stability via vector M_1 are the joints 18, 21, 25, i.e the vertical rotation of the upper body. The joints that have a strong contribution in stability via vector M_1 are the joints 5, 6, 7, 8, i.e the joints of the stance leg, the joints 17 and 19, i.e the motion of the torso in sagittal plane and the joint 13, thus the joint of the swing foot. The second group of joints has a strong contribution in the dynamics of the motion due to the large inertia and mass implied in their motion contrarily to the joint of the swing foot that affects directly the landing configuration, the first group of joints contributes via the dynamics and the landing configuration. The other joints have an intermediate effects on stability. The results are illustrated with the variation of $M_1(5)$ which allows to find a stable point, as shown in Fig. 8. We can see that if $M_1(5) = -1.5$, the walking will be stable. According to the definition of M_1 (see Eqs. (22) and (23)), this choice implies that the desired evolution of q_7 is now $q_7 = q_7^d(\theta) - 1.5(q_2^d(\theta) - q_2)$. The physical interpretation of this equation is that a change of q_2 to satisfy the condition on the position of the ZMP in the frontal plane will be done in synergy with a change on q_7.

6.4. Simulation results of the control law

The control law defined by $M_1(i) = 0, i \neq 5$ and $M_1(5) = -1.5$ is tested on the simulator with an initial error of 0.01 rad on the uncontrolled joint angle q_2 and a velocity error of 0.01 rad/s on $\dot{q}_2$ and $\dot{\theta}$. Errors on the other joints are introduced to have a double support configuration.

The studied walking including the foot rotation phase has been described in Fig. 2. The first three steps obtained in closed loop are illustrated in Fig. 9. Figure 10 shows that the heights of two vertices of the toe (P_1 and P_4 in Fig. 3) are the same, the heights of two vertices of the heel (P_2 and P_3) are also the same, that means both of the swing foot does not roll during the whole walking phase. In the fully support phase, the stance foot keeps flat on the ground, which is also indicated by Fig. 11 because it shows $ZMP = ZMP^d$. In the foot rotation phase, the stance foot rotates around its metatarsal axis in the sagittal plane as we desired until the impact phase. In Fig. 11, we have $ZMP = 0$. In Fig. 10, it can be observed that P_2 and P_3 take off before P_1 and P_4. At the same time, the sole of swing foot parallels with the ground just before impact, thus a good landing is obtained.

The tracking errors of two uncontrolled joints q_2, q_3 are shown in Fig. 12, where q_2 is an additional term in the controlled variable u, q_3 is a component of θ. The figures reveal that the tracking errors remain close to zero after vanishing of the initial error. The phase planes for $q_i, i = 2, 3, 4, 5$ are shown in Fig. 13. It shows that the walking converges to a periodic motion after some steps. In summary, the proposed control law produced a stable walking although the under-actuated phase exists.

https://doi.org/10.1017/S0263574713000866 Published online by Cambridge University Press

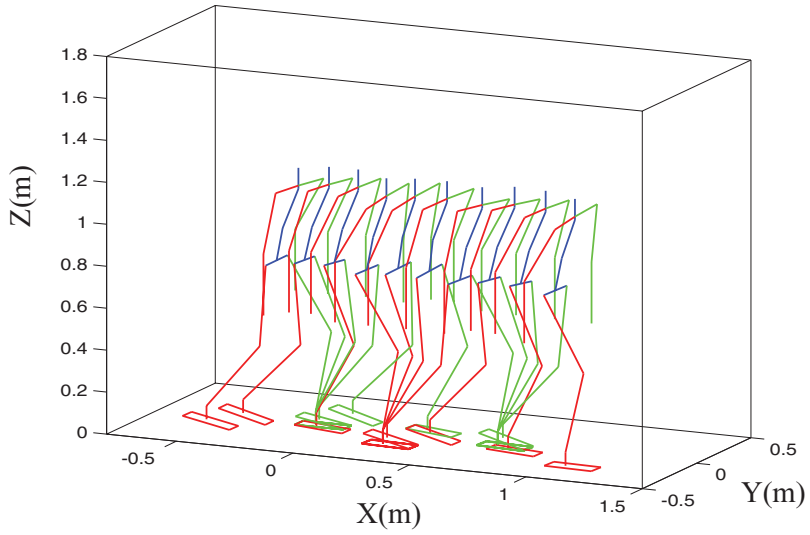


Fig. 9. (Colour online) The walking motion of the robot with the foot rotation phase during first three steps.

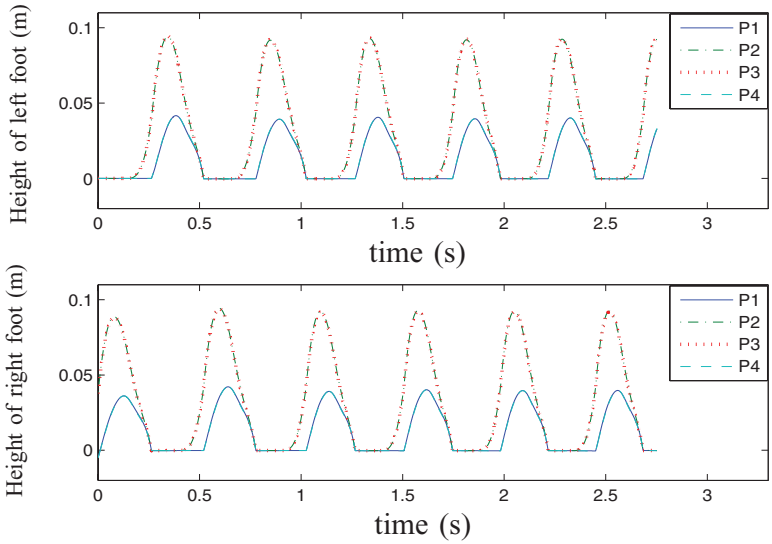


Fig. 10. (Colour online) Height of feet for the walking including the foot rotation phase.

6.5. Simulation results of the control law with modelling errors

In order to further verify the robustness of the control law, besides of the introduced initial errors, the modelling errors are also considered in the simulation. At first, all the inertial parameters are changed to -20% in the dynamic models of the control law. The simulation results are shown in Figs. 14 and 15. By comparing them with the previous results, the influence of modelling errors on the walking of biped robot can be clearly seen.

Since the inertial parameters in the control law are not the same as that in the simulator, there exist tracking errors of the desired ZMP and these errors are constant, see Fig. 15. The figure also shows that the position of ZMP is always within the limits of the foot sole so at least the robot can keep balance until the simulation stop. Figure 14 shows the tracking errors of q_2 and q_3, compare it with Fig. 12, it indicates that the tracking errors of the joint angles do not diverge although there exist modelling errors.

In general, the modelling errors are smaller, the converge properties of walking are better. However, the walking robustness also depends on the desired trajectory. If the margin of the desired ZMP is very small, the acceptable modelling errors are small too. For example, when all the inertial parameters are changed to $+10\%$, the resulted ZMP_x almost reaches the edge of the heel, as shown in Fig. 16.

https://doi.org/10.1017/S0263574713000866 Published online by Cambridge University Press

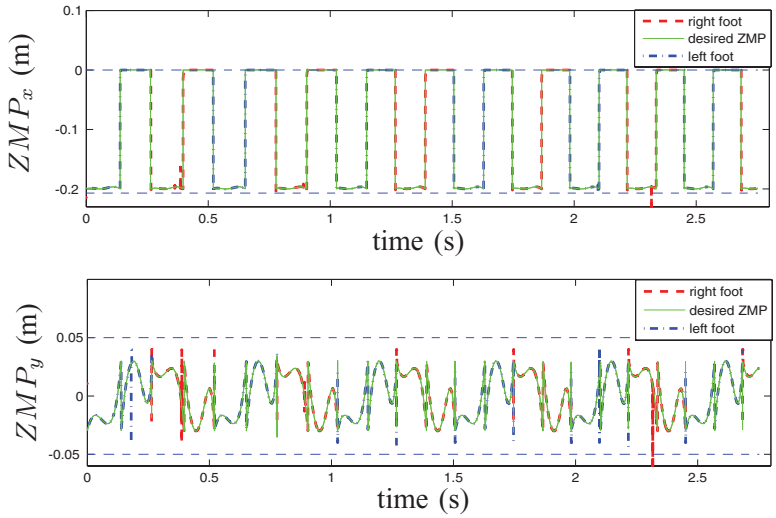


Fig. 11. (Colour online) Position of ZMP in the foot sole for the walking including the foot rotation phase: the position of ZMP moves periodically. ZMP_y is always within the limits and ZMP_x is zero during an under-actuated phase.

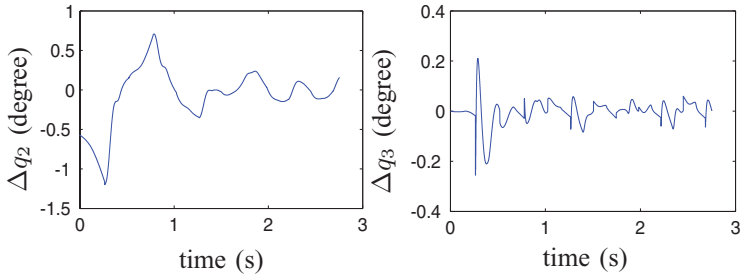


Fig. 12. (Colour online) The tracking errors of q_2 and q_3 for the walking including the foot rotation phase.

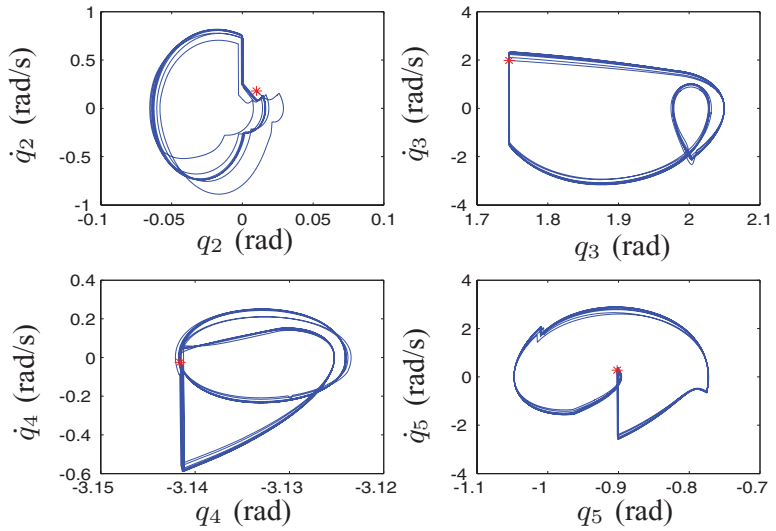


Fig. 13. (Colour online) Phase-plane plots for q_i, $i = 2, 3, 4, 5$ for the walking including the foot rotation phase. The initial state is represented by a (red) star.

https://doi.org/10.1017/S0263574713000866 Published online by Cambridge University Press

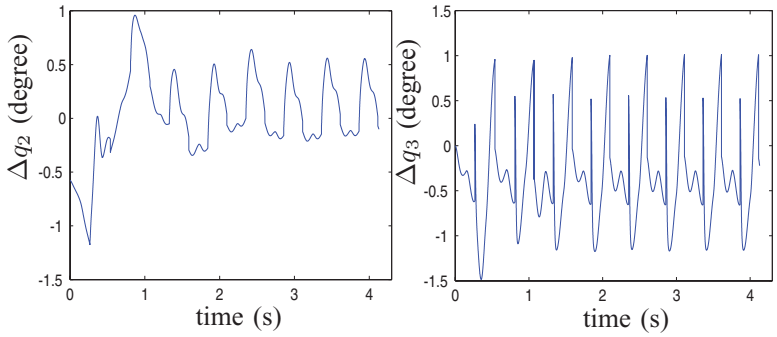


Fig. 14. (Colour online) The tracking errors of q_2 and q_3 for the proposed control law considering initial errors and -20% modelling errors.

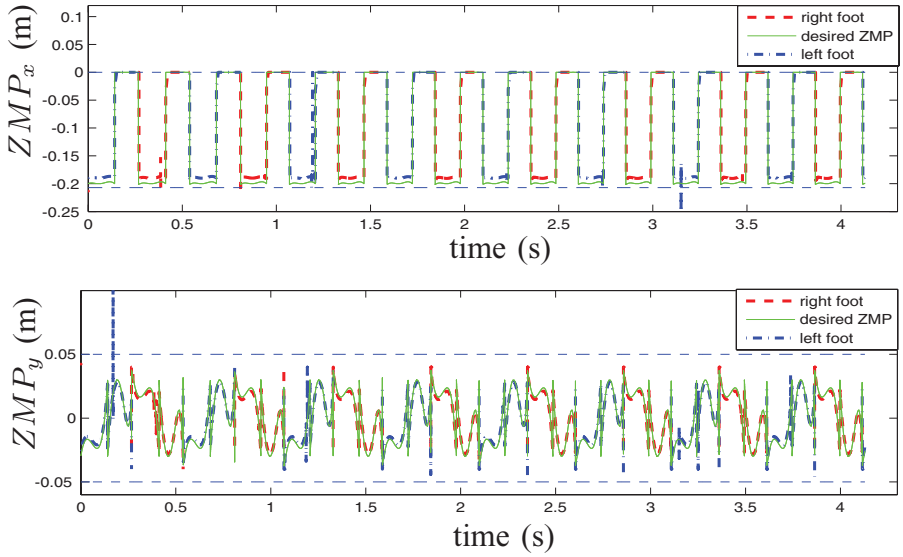


Fig. 15. (Colour online) Position of ZMP for the proposed control law considering initial errors and -20% modelling errors. ZMP_y is always within the limits and ZMP_x is zero during an under-actuated phase.

Luckily, the ZMP has not gotten out of the foot sole. However, we have tested that when the errors are changed to $+20\%$, the ZMP gets out of the foot sole certain times, thus the walking is no longer stable.

7. Conclusions

This paper proposed a walking control law for a 3D biped robot considering the foot rotation phase. The reference motion is parameterized as a reference path in the joint space in order to solve the problem of under-actuation during the foot rotation phase. The control law consists of a ZMP controller, a swing ankle rotation controller and a partial joint angles controller. Its objective is controlling the ZMP, the swing ankle rotation and the partial joints angles, simultaneously. By creating the hybrid zero dynamics, a stability study with application of the Poincaré method was evaluated in a reduced space. The influence of the controlled partial joints selection on the stability of the control law was investigated. The examples showed that the stability can be improved by a pertinent choice of the controlled partial joints.

It is worth mentioning that although the rotation angle of the stance foot is added in the overall joint configuration vector, the computed torque around the toe during the foot rotation phase is zero since the constraints on the ZMP position are taken into account. Therefore, the proposed dynamic

https://doi.org/10.1017/S0263574713000866 Published online by Cambridge University Press

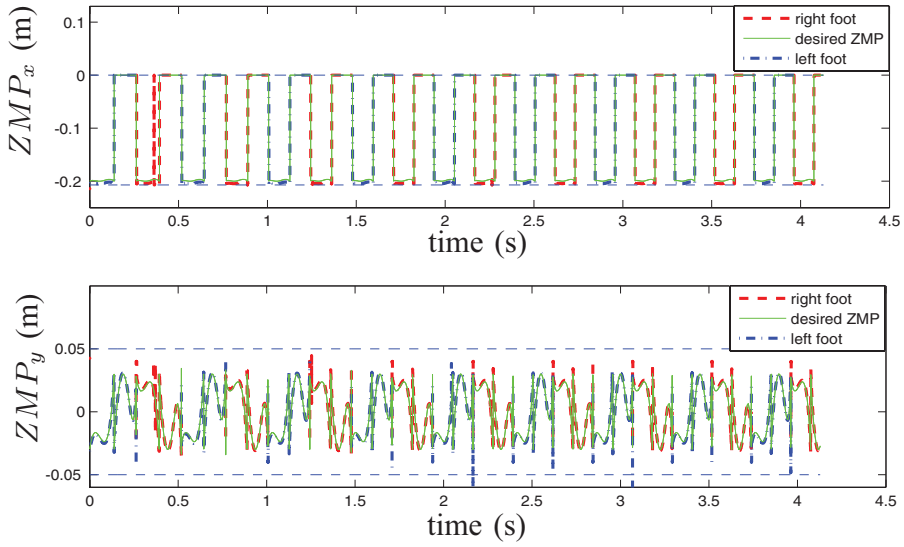


Fig. 16. (Colour online) Position of ZMP for the proposed control law considering initial errors and +10% modelling errors. ZMP_x almost reaches the edge of the heel during the fully support phase.

model in the foot rotation phase is still useful in the fully support phase because that can be viewed as a special case of that the foot rotation angle is zero. In addition, the proposed control law is suitable for both phases. The introduction of a finite double support phase will be considered soon.

In this study, a computed torque control law has been tested. Further study will consider simplification of this control law, to avoid the on-line calculation of the inverse dynamic model which can be time consuming. A classical joint control can be envisaged with a reference trajectory expressed as function of θ, measured on-line, and of q_2 which is adapted to satisfying the constraint on the ZMP. It can be remarked that the adaptation of q_2 will affect only the joint angles of the swing leg to have a good landing of the foot and the joint corresponding to a non-zero component in M_1 (in the case simulated, only a stance hip joint is concerned). The dynamic model involved in the control of the ZMP may also be simplified to reduce the computation cost.

Acknowledgements

This work is supported by ANR grants for the R2A2 project.

References

1. V. Acary and B. Brogliato, *Numerical Methods for Nonsmooth Dynamical Systems: Applications in Mechanics and Electronics*, ser. Lecture Notes in Applied and Computational Mechanics, vol. 35 (Springer-Verlag, Springer, 2008).
2. S. Alfayad, Robot humanoïde hydroïd: Actionnement, structure cinématique et stratègie de contrôle. *Ph.D. dissertation* (Université de Versailles Saint Quentin en Yvelines, 2009), in French.
3. C. Chevallereau, G. Abba, Y. Aoustin, F. Plestan, E. R. Westervelt, C. Canudas-de-wit and J. W. Grizzle, "Rabbit: A testbed for advanced control theory," *IEEE Control Syst.* **23**(5), 57–78 (2003).
4. C. Chevallereau, D. Djoudi and J. Grizzle, "Stable bipedal walking with foot rotation through direct regulation of the zero moment point," *IEEE Trans. Robot.* **24**(2), 390–401 (Apr. 2008).
5. C. Chevallereau, J. Grizzle and C. Shih, "Asymptotically stable walking of a five-link underactuated 3d bipedal robot," *IEEE Trans. Robot.* **25**(1), 37–50 (Feb. 2009).
6. S. Coros, P. Beaudoin and M. van de Panne, "Generalized biped walking control," *ACM Trans. Graph.* **29**(4), article 130 (Jul. 2010).
7. J. Ferreira, M. Crisostomo and A. Coimbra, "Neuro-Fuzzy zmp Control of a Biped Robot," *Proceedings of the 6th WSEAS International Conference on Simulation, Modeling and Optimization*, Lisbon, Portugal (Sep. 2006) pp. 331–337.
8. D. Goswami and P. Vadakkepat, "Planar bipedal jumping gaits with stable landing," *IEEE Trans. Robot.* **25**(5), 1030–1046 (2009).

https://doi.org/10.1017/S0263574713000866 Published online by Cambridge University Press

9. J. Grizzle, G. Abba and F. Plestan, "Asymptotically stable walking for biped robots: Analysis via systems with impulse effects," *IEEE Trans. Autom. Control* **46**, 51–64 (Jan. 2001).
10. K. Hirai, M. Hirose, Y. Haikawa and T. Takenaka, "The Development of Honda Humanod Robot," *Proceedings of the IEEE International Conference on Robotics and Automation*, Leuven, Belgium (1998), pp. 1321–1326.
11. Q. Huang, K. Kaneko, K. Yokoi, S. Kajita, T. Kotoku, N. Koyachi, H. Arai, N. Imamura, K. Komoriya and K. Tanie, "Balance Control of a Biped Robot Combining Off-Line Pattern with Real-Time Modification," *Proceedings of International Conference on Robotics and Automation*, San Francisco, USA (2000), pp. 3346–3352.
12. Q. Huang, K. Yokoi, S. Kajita, K. Kaneko, H. Arai, N. Koyachi and K. Tanie, "Planning walking patterns for a biped robot," *IEEE Trans. Robot. Autom.* **17**(3), 280–289 (2001).
13. S. Hyon, N. Yokoyama and T. Emura, "Back handspring of a multi-link gymnastic robot - reference model approach," *Adv. Robot.* **20**(1), 93–113 (2006).
14. A. Isidori, *Nonlinear Control Systems*, 3rd ed. (Springer-Verlag, Berlin, 1995).
15. S. Kajita, F. Kanehiro, K. Kaneko, K. Fujiwara, K. Harada, K. Yokoi and H. Hirukawa, "Biped walking pattern generator allowing auxiliary zmp control," *Proceedings of the 2006 IEEE/RSJ International Conference on Intelligent Robots and Systems*, Beijing, China (Oct. 2006) pp. 2993–2999.
16. S. Kajita, K. Kaneko, M. Morisawa, S. Nakaoka and H. Hirukawa, "Zmp-Based Biped Running Enhanced by Toe Springs," *Proceedings of the IEEE International Conference on Robotics and Automation*, Roma, Italy (2007) pp. 3963–3969.
17. S. Kajita, O. Matsumoto and M. Saigo, "Real-Time 3d Walking Pattern Generation for a Biped Robot with Telescopic Legs," *Proceedings of International Conference on Robotics and Automation*, Seoul, Korea (May 2001) pp. 2299–2306.
18. S. Kajita, M. Morisawa, K. Harada, K. Kaneko, F. Kanehiro, K. Fujiwara and H. Hirukawa, "Biped Walking Pattern Generation by Using Preview Control of Zero-Moment Point," *Proceedings of the ICRA '03 IEEE International Conference on Robotics and Automation*, Taipei, Taiwan (Sep. 2003) pp. 1620–1626.
19. W. Khalil and E. Dombre, *Modeling, Identification and Control of Robots* (Hermes Sciences, Paris, Europe, 2002).
20. J. Kim, I. Park and J. Oh, "Experimental realization of dynamic walking of the biped humanoid robot khr-2 using zero moment point feedback and inertial measurement," *Adv. Robot.* **20**(6), 707–736 (2006).
21. A. Kuo, "Energetics of actively powered locomotion using the simplest walking model," *J. Biomech. Eng.* **124**, 113–120 (2002).
22. J. Luh, M. Walker and R. Paul, "On line computational scheme for mechanical manipulators," *Trans. ASME, J. Dyn. Syst. Meas. Control* **102**(2), 69–76 (1980).
23. K. Mitobe, G. Capi and Y. Nasu, "Control of walking robots based on manipulation of the zero moment point," *Robotica* **18**, 651–657 (2000).
24. B. Morris and J. Grizzle, "Hybrid invariant manifolds in systems with impulse effects with application to periodic locomotion in bipedal robots," *IEEE Trans. Autom. Control* **54**(8), 1751–1764 (2009).
25. H. Nijmeijer and A. van der Schaft, *Nonlinear Control Dynamical Systems* (Springer-Verlag, Berlin, 1989).
26. F. Plestan, J. Grizzle, E. Westervelt and G. Abba, "Stable walking of a 7-dof biped robot," *IEEE Trans. Robot. Autom.* **19**(4), 653–668 (2003).
27. C. Rengifo, Y. Aoustin, F. Plestan and C. Chevallereau, "Contact Forces Computation in a 3D Bipedal Robot Using Constrained-Based and Penalty-Based Approaches," *Proceedings of Multibody Dynamics*, Bruxelle, Belgium (CDROM) (2011).
28. T. Sugihara, Y. Nakamura and H. Inoue, "Realtime Humanoid Motion Generation Through zmp Manipulation Based on Inverted Pendulum Control," *Proceedings of the IEEE International Conference on Robotics and Automation* Washington, DC (2002) pp. 1404–1409.
29. T. Takahashi and A. Kawamura, "Posture Control for Biped Robot Walk with Foot Toe and Sole," **In**: *27th Annual Conference of the IEEE Industrial Electronics Society* Denver, CO (2001) pp. 329–334.
30. H. Takeuchi, "Development of 'mel horse'," *Proceedings of International Conference on Robotics and Automation*, Seoul, Korea (May 2001) pp. 3165–3171.
31. D. Tlalolini, Y. Aoustin and C. Chevallereau, "Design of a walking cyclic gait with single support phases and impacts for the locomotor system of a thirteen-link 3d biped using the parametric optimization," *Multibody Syst. Dyn.* **23**(1), 33–56 (2010).
32. D. Tlalolini, C. Chevallereau and Y. Aoustin, "Comparison of different gaits with rotation of the feet for a planar biped," *Robot. Auton. Syst.* **57**(4), 371–383 (2009).
33. D. Tlalolini, C. Chevallereau and Y. Aoustin, "Human-like walking: Optimal motion of a bipedal robot with toe-rotation motion," *IEEE/ASME Trans. Mechatronics* **16**(2), 310–320 (2011).
34. M. Vukobratovic, B. Borovac, D. Surla and D. Stokic, *Biped Locomotion - Dynamics, Stability, Control and Application* (Springer-Verlag, Berlin, 1990).
35. T. Wang, Study of Walking Control for Biped Robots, *Ph.D. dissertation* (Nantes, France: Ecole Centrale de Nantes, Dec. 2011).
36. T. Wang and C. Chevallereau, "Stability analysis and time-varying walking control for an under-actuated planar biped robot," *Robot. Auton. Syst.* **59**(6), 444–456 (2011).

https://doi.org/10.1017/S0263574713000866 Published online by Cambridge University Press

37. T. Wang, C. Chevallereau and C. Rengifo, "Walking and steering control for a 3D biped robot considering ground contact and stability," *Robot. Auton. Syst.* **60**(7), 962–977 (2012).
38. E. Westervelt, J. Grizzle and D. Koditschek, "Hybrid zero dynamics of planar biped walkers," *IEEE Trans. Autom. Control* **48**(1), 42–56 (2003).
39. E. Westervelt, J. Grizzle, C. Chevallereau, J. Choi and B. Morris, *Feedback Control of Dynamic Bipedal Robot Locomotion*, ser. Control and Automation (CRC Press, Boca Raton, Jun. 2007).
40. K. Yi, "Walking of a Biped Robot with Compliant Ankle Joints: Implementation with Kubca," *Proceedings of the 39th IEEE Conference Decision and Control*, Sydney, Australia (Dec. 2000) pp. 4809–4814.

https://doi.org/10.1017/S0263574713000866 Published online by Cambridge University Press